ORGANOMETALLICS

pubs.acs.org/Organometallics Article

Isomerization-Induced Multiple Reaction Pathways in Platinum-Catalyzed C−H Acylation Reaction of 2-Aryloxypyridines

Alexander Barham,[§] Justin Neu,[§] Cathleen L. Canter, Robert D. Pike, Yumin Li, and Shouquan Huo*

Cite This: *Organometallics* 2021, 40, 3158−3169 Read Online

ACCESS | Metrics & More | Article Recommendations | Supporting Information

ABSTRACT: In Pt-catalyzed C−H acylation of 2-(2-methylphenoxy)pyridine (L^1) with ethyl chlorooxoacetate to produce ethyl 2-(3-methyl-2-(pyridin-2-yloxy))phenyl-2-oxoacetate (L^2), possible reaction steps involved in the catalytic cycle have been investigated, which include the ligand exchange of precatalysts *cis*- and *trans*-$Pt(PhCN)_2Cl_2$ with L^1, the intramolecular C−H activation (cyclometalation) of *cis*- and *trans*-$Pt(L^1)_2Cl_2$ (**1**), and the acylation of the *trans*-cyclometalated platinum complex (*trans*-**2**) formed from the C−H activation reaction. The *cis* coordination compounds including the intermediate platinum complexes have shown much higher reactivity toward the ligand exchange and the C−H activation than their *trans* isomers. Consequently, the *cis* isomers exhibit higher catalytic activity in the C−H acylation reaction. Although the C−H activation of *cis*- and *trans*-$Pt(L^1)_2Cl_2$ produces *trans*-**2**, the *cis* isomer (*cis*-**2**) is very likely formed in the C−H activation of *cis*-$Pt(L^1)_2Cl_2$ but undergoes isomerization to the more stable *trans*-**2**. The results suggest that the fast reaction pathway via all *cis*-platinum complexes may be responsible for the efficient catalytic reaction, but isomerization of *cis*-**2** to *trans*-**2** could be highly competitive. The acylation of the *trans*-cycloplatinated complex produces both *cis*- and *trans*-platinum complexes $Pt(L^1)(L^2)Cl_2$. The regaining of the *cis*-platinum complex revives the catalytic cycle.

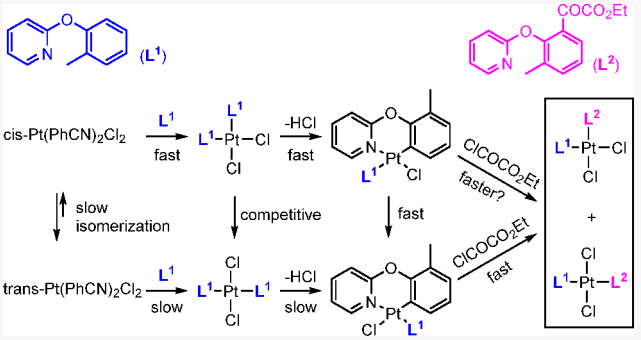

INTRODUCTION

Platinum plays an important role in the development of transition-metal-catalyzed C−H activation and functionalization reactions.[1] The ligand-directed transition-metal-catalyzed C−H functionalization represents an important advancement in modern organic synthesis,[2] which usually involves the formation of an intermediate cyclometalated complex followed by the functionalization of the carbon−metal bond. Cyclometalated platinum complexes are very stable, and in fact, some cyclometalated platinum complexes are so stable that they have been used as phosphorescent materials in the fabrication of OLED (organic light-emitting diode) devices by vapor deposition.[3] Therefore, it is very difficult to functionalize a cycloplatinated complex[4] and construct a catalytic cycle for the C−H functionalization. In an early report, platinum was shown to catalyze *ortho*-silylation of benzylideneamines, and the reaction was believed to proceed through a cyclometalated platinum intermediate.[5] Recently, we discovered the acylation of cycloplatinated complexes derived from tridentate cyclometalating ligands 6-arylamino-2,2′-bipyridine, 6-phenoxy-2,2′-bipyridine, 6-phenylthio-2,2′-bipyridine, and 6-benzyl-2,2′-bipyridine.[6] Based on the discovery, we developed an oxidant- and additive-free, platinum-catalyzed ligand-directed C−H acylation reaction of 2-aryloxypyridines,[7] which provides an efficient way to introduce an acyl group to the *ortho*-position of the 2-aryloxypyridines and allow the synthesis of aryl aryl ketones,[7a] aryl alkyl ketones,[7a] *α,β*-unsaturated ketones,[7a] *α*-keto esters,[7b] and *γ*-keto esters[7b] (Scheme 1). The reaction is believed to proceed through two distinct steps: cycloplatination (C−H activation) and acylation of the platinacycle (functionalization). It was also noted that the precatalyst *cis*-

Scheme 1. Platinum-Catalyzed C−H Acylation of 2-Aryloxypyridines[7]

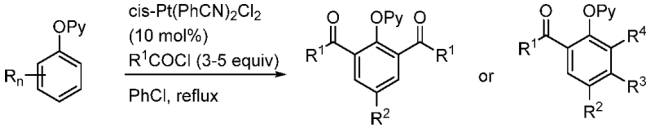

Py = 2-pyridyl
R^1 = alkyl, cycloalkyl, alkenyl, aryl, heteroaryl, CO_2Et, $CH_2CH_2CO_2Et$
R^2 = MeO, Me, H, Cl, Br
R^3 = MeO, Me, H, Cl, Br, CO_2Et.
R^4 = MeO, Me, H, Cl, CO_2Et, CN, NO_2

Received: June 23, 2021
Published: September 3, 2021

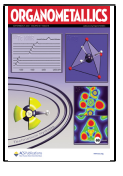

https://doi.org/10.1021/acs.organomet.1c00377
Organometallics 2021, 40, 3158−3169

$Pt(PhCN)_2Cl_2$ exhibited catalytic activity higher than that of *trans*-$Pt(PhCN)_2Cl_2$.[7b] To deepen our understanding of this interesting catalytic reaction, especially the difference in the catalytic activity of two isomeric platinum complexes, we decided to investigate a series of stoichiometric reactions including the ligand exchange, cycloplatination, and the acylation of the cycloplatinated compound, which could construct the catalytic cycle and provide insights into the reaction mechanism.

RESULTS AND DISCUSSION

Comparison of Catalytic Activity of *cis*- and *trans*-$Pt(PhCN)_2Cl_2$. A previous study showed that the *cis*-$Pt(PhCN)_2Cl_2$-catalyzed C−H acylation of 2-(naphthalen-2-yloxy)pyridine with ethyl chlorooxoacetate led to 80% conversion in 1 h (reflux in chlorobenzene); however, the use of *trans*-$Pt(PhCN)_2Cl_2$ as the catalyst achieved only about 30% conversion under the same conditions.[7b] To further substantiate this difference in catalytic activity, we monitored the product buildup with the reaction time for the reactions catalyzed by the two isomeric platinum complexes. We chose 2-(2-methylphenoxy)pyridine ($\mathbf{L^1}$) as the model substrate for the investigation because the presence of the methyl group provides a convenient way to monitor the reaction and quantify the product formation through analyzing the proton NMR spectra of the crude reaction mixture. As shown in eq 1,

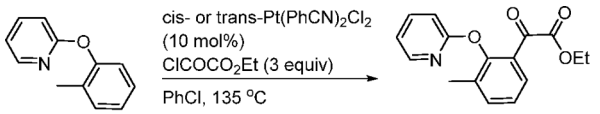

$\mathbf{L^1}$ $\mathbf{L^2}$ (1)

in the presence of a catalytic amount of $Pt(PhCN)_2Cl_2$, $\mathbf{L^1}$ can be converted into the α-keto ester ($\mathbf{L^2}$)[7b] through *ortho*-C−H acylation reaction with ethyl chlorooxoacetate. To compare the catalytic activity of *cis*- and *trans*-$Pt(PhCN)_2Cl_2$, two parallel reactions were performed using two different catalysts, and the reactions were monitored by periodically sampling the reaction mixture for proton NMR analysis. It should be mentioned that, for an accurate analysis, the crude reaction mixture was treated with an excess amount of pyridine to free any of 2-aryloxypyridine ligands ($\mathbf{L^1}$ and/or $\mathbf{L^2}$) from the platinum before taking the NMR spectra. The comparison of the catalytic activity is shown in Figure 1. The results clearly demonstrated that the *cis*-$Pt(PhCN)_2Cl_2$-catalyzed C−H acylation reaction was remarkably faster, especially in the initial stage of the reaction. With *cis*-$Pt(PhCN)_2Cl_2$ as the catalyst, the acylated product $\mathbf{L^2}$ was formed in 25, 51, and 74% yield within 15, 30, and 60 min, respectively. However, when *trans*-$Pt(PhCN)_2Cl_2$ was used as the catalyst, the product was formed in only 5, 15, and 28%, respectively. Interestingly, after 3 h, the yields of the product were comparable, 89 and 80% for *cis*- and *trans*-$Pt(PhCN)_2Cl_2$-catalyzed reactions, respectively. Prolonged reaction resulted in product degradation, which was also observed previously and has been attributed to the HCl accumulated during the reaction or the combination of HCl and platinum species.[7b]

To gain a deeper insight into this difference in catalytic activity and other aspects of the reaction mechanism, it is necessary to investigate a series of stoichiometric reactions that are likely involved in the catalytic cycle. As shown in Scheme 2, the Pt-catalyzed C−H acylation reaction most likely proceeds

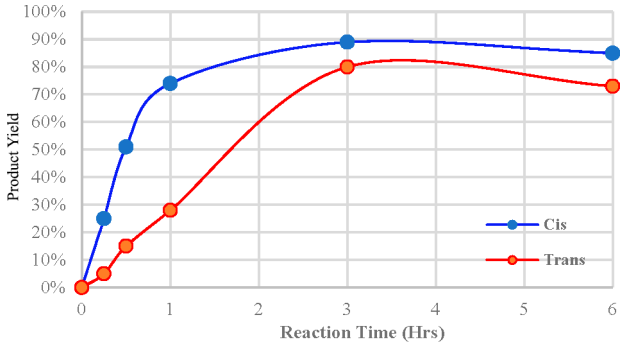

Figure 1. Comparison of catalytic activity of *cis*- and *trans*-$Pt(PhCN)_2Cl_2$. Data reported are based on single runs. For ease of readability, a smooth curve is added to connect the points using a graphing program but not intended to suggest any accurate kinetic features of the reaction.

through the exchange of the benzonitrile ligands of *cis*- or *trans*-$Pt(PhCN)_2Cl_2$ with the substrate $\mathbf{L^1}$ to form the coordination complex **1**, followed by the intramolecular C−H activation/cycloplatination to produce the cyclometalated compound **2** and the subsequent acylation of the cycloplatinated compounds to produce the coordination compounds **3**, which would enter into the next catalytic cycle through ligand exchange with $\mathbf{L^1}$ and release the product $\mathbf{L^2}$. For each possible intermediate platinum complex, there are two possible configurational isomers, namely, *trans* and *cis* isomers, depending upon the specific arrangement of the two N donors. Our study will be focused on characterizing these configurational isomers and comparing their chemical reactivities.

Reaction of 2-(2-Methylphenoxy)pyridine ($\mathbf{L^1}$) with *cis*- and *trans*-$Pt(PhCN)_2Cl_2$. Our initial study was to examine if a cycloplatinated complex would be formed under the conditions used in the catalytic reaction (reflux in chlorobenzene). Indeed, the reaction of $\mathbf{L^1}$ with *cis*-$Pt(PhCN)_2Cl_2$ proceeded smoothly in chlorobenzene at reflux, and all of *cis*-$Pt(PhCN)_2Cl_2$ was consumed after 2−3 h. The reaction produced a mixture of a coordination complex $Pt(\mathbf{L^1})_2Cl_2$ (**1**) and a cycloplatinated complex (**2**), which turned out to be *trans*-**1** and *trans*-**2**, in 41 and 42% isolated yield, respectively (Scheme 3). When *trans*-$Pt(PhCN)_2Cl_2$ was used, the reaction also produced a mixture of *trans*-**1** and *trans*-**2** in 45 and 32% yield, respectively. The cycloplatination reaction is reversible. While heating *trans*-**1** in chlorobenzene at reflux gave a mixture of *trans*-**1** and *trans*-**2**, the cycloplatinated complex *trans*-**2** underwent complete protonolysis to give *trans*-**1** when treated with an excess amount of HCl. In fact, the coordination complex *trans*-**1** can be conveniently prepared in 82% yield from the reaction of *cis*-$Pt(PhCN)_2Cl_2$ with $\mathbf{L^1}$ in the presence of HCl (Scheme 4). It can be reasoned that the addition of a HCl scavenger should drive the cycloplatination to completion. Indeed, in the presence of K_2CO_3, the reaction of $\mathbf{L^1}$ with *cis*-$Pt(PhCN)_2Cl_2$ in chlorobenzene at reflux for 2 h produced *trans*-**2** in 64% isolated yield. No coordination complex was presented in the final reaction mixture.

The structure of *trans*-**2** was determined by X-ray crystallography, and the *trans* relationship of the pyridine N donors was confirmed (Figure 2). The attempt to grow a suitable crystal of coordination complex *trans*-**1** for X-ray structure determination was unsuccessful. To determine the

https://doi.org/10.1021/acs.organomet.1c00377
Organometallics 2021, 40, 3158−3169

Scheme 2. Possible Reaction Steps Involved in the Pt-Catalyzed C−H Acylation of L^1

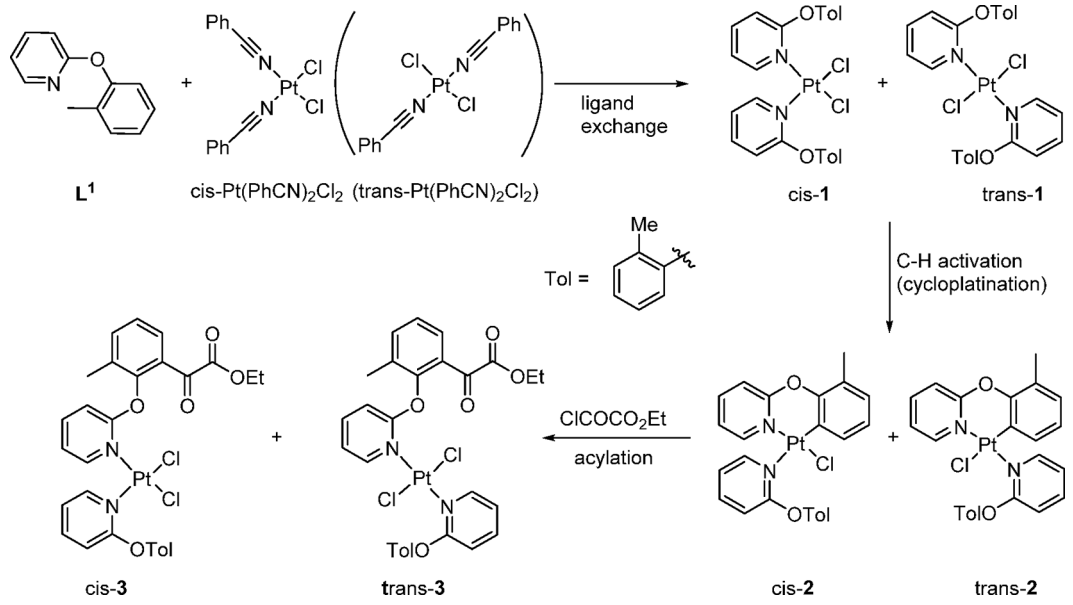

Scheme 3. Reaction of L^1 with $Pt(PhCN)_2Cl_2$

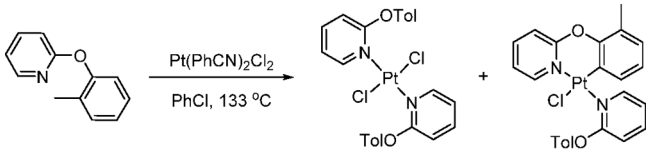

Scheme 4. Synthesis of *trans*-1 and *trans*-4

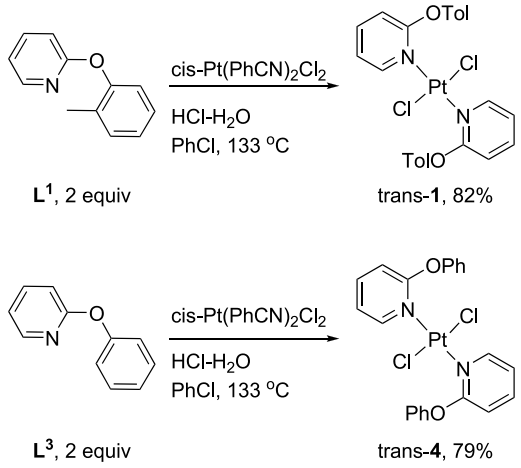

structure of the coordination complex, we decided to make a similar complex using a different substrate. As expected, the reaction of 2-phenoxypyridine (L^3) with *cis*-$Pt(PhCN)_2Cl_2$ in the presence of HCl also produced *trans*-**4** in good yield (Scheme 4), and fortunately, the structure of *trans*-**4** was successfully determined by X-ray crystallography. The formation of *cis* coordination complexes *cis*-**1** and *cis*-**4** was not detected under these reaction conditions. Instead, *cis*-**1** and *cis*-**4** were prepared by reacting 2-aryloxypyridines L^1 and L^3, respectively, with K_2PtCl_4 in water/acetic acid at room temperature (Scheme 5). The reactions produced exclusively the *cis* isomers and were obviously under kinetic control. Interestingly, attempting to grow crystals of *cis*-**1** for X-ray was unsuccessful, but suitable crystals of *cis*-**4** were successfully prepared for X-ray structure determination. The molecular structures of *trans*-**2**, *trans*-**4**, and *cis*-**4** are shown in Figure 2. The crystal data and refinement parameters are listed in Tables S1−S3 (Supporting Information). The selected bond lengths and angles relevant to the platinum coordination sphere are listed in Table 1.

The platinum in *trans*-**2** adopts a square-planar geometry typically found in a Pt(II) complex. The Pt−N(1) (cyclometalated ligand) is slightly shorter (by 0.026 Å) than the Pt−N(2) (coordinating ligand) bond. The six-membered metallacycle exhibits a boat-like conformation with the oxygen and the platinum being the two flagpoles, which is similar to the structure of a cyclometalated palladium complex formed with an aryl heteroaryl ether[8] and other cycloplatinated complexes based on the aryl heteroaryl amine ligand[9] or six-membered coordination platinum complexes based on N- or C-linked bis(pyridine) ligands.[10] The distances from Pt and O atoms to the boat-bottom plane defined by the four atoms C(5)C(6)-C(7)N(1) are 0.826 and 0.498 Å, respectively. The lengths of Pt−C and Pt−N bonds are similar to those found in the six-membered cycloplatinated complexes.[11] The Pt−Cl bond (2.4121(6) Å) is longer than a normal Pt−Cl (in the range of 2.30−2.33 Å).[12] This is due to the influence of the stronger carbon donor which is *trans* to the chloride.[13]

For both coordination complexes *trans*- and *cis*-**4**, the platinum displays a nearly perfect square-planar geometry, which is similar to the crystal structures of *cis*- and *trans*-dichlorobispyridine platinum complexes reported previously.[14] Although the two organic ligands in *trans*-**4** are placed symmetrically with Pt as the inversion center, the *cis*-**4** has two coordinating ligands arranged unsymmetrically, which is obviously due to the steric effect. In both structures, the coordinating pyridyl rings are twisted from the square-planar Pt coordination planes. The lengths of the two Pt−N bonds are slightly different. There is a distinct feature of the ^1H NMR spectra of *cis* and *trans* coordination complexes **1** and **4**, which is the difference in chemical shifts of the *ortho* protons of the

https://doi.org/10.1021/acs.organomet.1c00377
Organometallics 2021, 40, 3158−3169

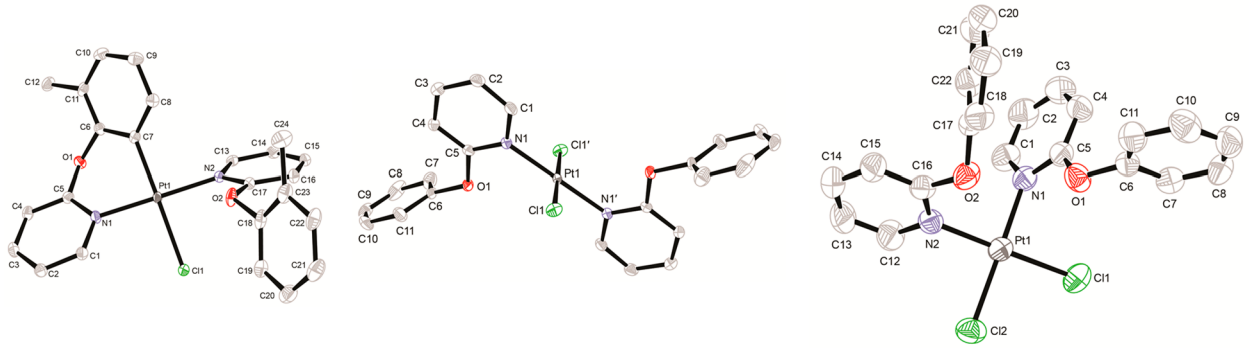

Figure 2. ORTEP diagram of complexes *trans*-**2** (left), *trans*-**4** (middle), and *cis*-**4** (right) shown with thermal ellipsoids given at the 50% probability level. Hydrogen atoms are omitted for clarity.

Scheme 5. Synthesis of *cis*-1 and *cis*-4

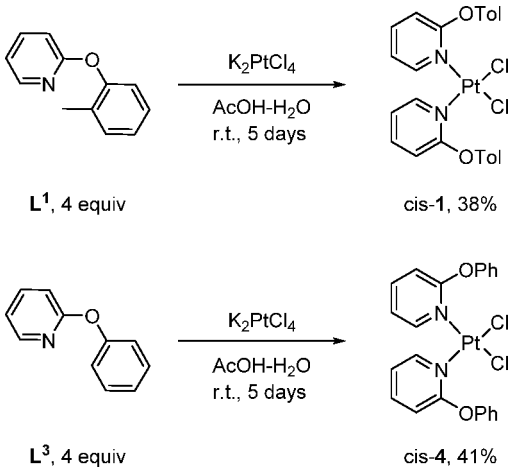

phenyl rings in the ligands $\mathbf{L}^1$ and $\mathbf{L}^3$ of the coordination complexes. The signals of the *cis* isomer appear at a significantly lower frequency compared to those of the *trans* isomers (about 0.5 ppm in difference). By reviewing the crystal structure, it was discovered that the *ortho* protons of one coordination ligand in *cis*-**4** are located above an aromatic ring of the other coordination ligand, either the pyridyl ring or the phenyl ring, therefore in the shielding region. The distances of the hydrogens to the aromatic plane are 3.03 and 2.946 Å, respectively (Figure 3), indicative of CH/π interaction.[15] This distinct feature can help us to assign the configuration of other similar platinum coordination complex with 2-aryloxypyridine ligands.

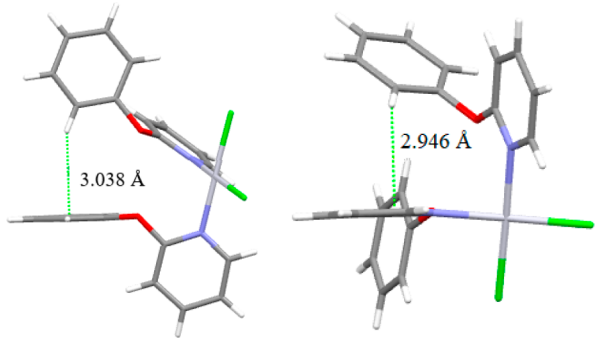

Figure 3. Distances of the *ortho*-hydrogen atoms to the aromatic ring planes in *cis*-**4**.

Ligand Exchange of $\mathbf{L}^1$ with $Pt(PhCN)_2Cl_2$. The reaction of $\mathbf{L}^1$ and $Pt(PhCN)_2Cl_2$ in chlorobenzene at reflux was under thermodynamic control, and the C−H activation/cyclometalation occurred readily under those conditions, which provided very limited information about the ligand exchange step. Therefore, we investigated the ligand exchange reaction at a lower temperature using 1,2-dichloroethane (DCE) as the solvent, hoping that the C−H activation would be minimum at reflux in DCE. As expected, the ligand exchange with *cis*-$Pt(PhCN)_2Cl_2$ proceeded smoothly for the first hour to produce a mixture of mainly the coordination complex *cis*-**1**, a small amount of *trans*-**1**, *trans*-**2**, and monosubstituted platinum complex *trans*-$Pt(\mathbf{L}^1)(PhCN)Cl_2$ (*trans*-**5**) in a ratio of 66:15:8:11 and combined yield of 90% (Table 2), along with a small amount of other unidentified products. Complex *cis*-**1** was produced in 60% yield. In contrast, in the reaction with *trans*-$Pt(PhCN)_2Cl_2$, the formation of *trans*-**1** is

Table 1. Bond Lengths (Å) and Angles (deg) for Compounds *trans*-2, *trans*-4, and *cis*-4

trans-**2**		*trans*-**4**		*cis*-**4**	
Pt(1)−C(7)	1.988(2)	Pt(1)−N(1)′	2.0311(19)	Pt(1)−N(1)	2.034(5)
Pt(1)−N(1)	2.011(2)	Pt(1)−N(1)	2.0311(19)	Pt(1)−N(2)	2.041(5)
Pt(1)−N(2)	2.037(2)	Pt(1)−Cl(1)	2.3030(6)	Pt(1)−Cl(2)	2.2989(16)
Pt(1)−Cl(1)	2.4121(6)	Pt(1)−Cl(1)′	2.3030(6)	Pt(1)−Cl(1)	2.3000(16)
C(7)−Pt(1)−N(1)	86.93(9)	N(1)′−Pt(1)−N(1)	180.00(10)	N(1)−Pt(1)−N(2)	90.36(19)
C(7)−Pt(1)−N(2)	92.69(9)	N(1)′−Pt(1)−Cl(1)	91.13(6)	N(1)−Pt(1)−Cl(2)	177.40(13)
N(1)−Pt(1)−N(2)	177.25(8)	N(1)−Pt(1)−Cl(1)	88.87(6)	N(2)−Pt(1)−Cl(2)	89.41(14)
C(7)−Pt(1)−Cl(1)	176.90(7)	N(1)′-Pt(1)−Cl(1)′	88.87(6)	N(1)−Pt(1)−Cl(1)	88.37(14)
N(1)−Pt(1)−Cl(1)	92.12(6)	N(1)−Pt(1)−Cl(1)′	91.13(6)	N(2)−Pt(1)−Cl(1)	177.89(14)
N(2)−Pt(1)−Cl(1)	88.11(6)	Cl(1)−Pt(1)−Cl(1)′	179.999(16)	Cl(2)−Pt(1)−Cl(1)	91.79(7)

https://doi.org/10.1021/acs.organomet.1c00377
Organometallics 2021, 40, 3158−3169

Table 2. Product Yields and Distribution for Ligand Exchange Reactions of L^1 with *cis*- and *trans*-$Pt(PhCN)_2Cl_2$[a]

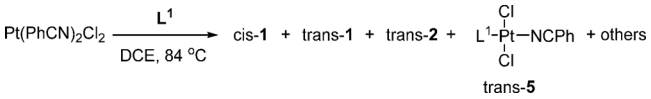

reagents	*cis*-$Pt(PhCN)_2Cl_2$					*trans*-$Pt(PhCN)_2Cl_2$				
products	*cis*-**1**	*trans*-**1**	*trans*-**2**	*trans*-**5**	total	*cis*-**1**	*trans*-**1**	*trans*-**2**	*trans*-**5**	total
1 h	60%	14%	6%	10%	90%	19%	5%	8%	38%	70%
2 h	67%	16%	4%	9%	96%					
3 h	67%	19%	4%	10%	100%	33%	9%	9%	40%	91%
8 h	63%	21%	7%	9%	100%	33%	14%	15%	34%	96%
22 h						24%	27%	32%	15%	98%

[a]Conditions: $Pt(PhCN)_2Cl_2$ (1 molar equiv), ligand L^1 (3.4 molar equiv), DCE (2 mL), 84 °C. The yields were estimated by analyzing ^1H NMR spectra of crude reaction mixtures, and the calculations were based on the integrations of the 6-Hs of the pyridine rings, which appear in the high-frequency region and are isolated from all other hydrogen atoms in the complexes, the ligand, and the solvent (Figures S10 and S11).

much slower. The major product is monosubstituted complex *trans*-**5**, which was formed in 38% yield within 1 h, along with *cis*-**1**, *trans*-**1**, and *trans*-**2** in 19, 5, and 8% yield, respectively. The yield of *cis*-**1** was only increased to 33% after 3 h, with 40% of monosubstituted complex *trans*-**5**. Prolonged reaction led to the accumulation of *trans*-**1** and *trans*-**2**.

Several points can be noted from the data in the Table 2. First, the ligand exchange of *cis*-$Pt(PhCN)_2Cl_2$ with L^1 is much faster than that of its *trans* isomer. In particular, the further ligand substitution of *trans*-**5** with L^1 is very slow. Second, the intramolecular C−H activation of both *cis*-**1** and *trans*-**1** is very slow, as the amount of *trans*-**2** in the reactions did not increase much. Third, the isomerization of *cis*-**1** to *trans*-**1** is very sluggish, too, as the yield of *cis*-**1** remained nearly constant during 8 h of monitoring the reaction of *cis*-$Pt(PhCN)_2Cl_2$ with L^1. Finally, the reaction appeared to be stereoselective but not specific since both reactions of *cis*- and *trans*-$Pt(PhCN)_2Cl_2$ produced more *cis*-**1** than *trans*-**1**. Square-planar 16-e Pt(II) complexes undergo associative ligand exchange, and most of the reactions proceed with the retention of the configuration, namely, stereospecifically.[16] In cases where a change of the configuration is observed such as isomerization of a square-planar Pt(II) complex, pseudorotation of a five-coordinate intermediate has been proposed as the most likely cause of the configuration change.[17] However, this isomerization cannot explain the predominate formation of *cis*-**1** over *trans*-**1** in the reaction of *trans*-$Pt(PhCN)_2Cl_2$, as the *trans*-**1** should be more stable than *cis*-**1**. A possible reason might be that the formation of *cis*-**1** in the reaction of *trans*-$Pt(PhCN)_2Cl_2$ was through an isomerization of *trans*-$Pt(PhCN)_2Cl_2$ to *cis*-$Pt(PhCN)_2Cl_2$ followed by the stereospecific ligand exchange (eq 2). There have been reports of an equilibrium between *cis*- and *trans*-$Pt(PhCN)_2Cl_2$ in solution.[18]

$$\textit{trans}\text{-}Pt(PhCN)_2Cl_2 \rightleftarrows \textit{cis}\text{-}Pt(PhCN)_2Cl_2 \xrightarrow{L^1} \textit{cis}\text{-}\mathbf{1} \qquad (2)$$

The structure of monosubstituted complex *trans*-**5** was determined by X-ray crystallography (Figure 4). The crystal data and refinements parameters are listed in Table S4 (Supporting Information). There are two independent molecules, *trans*-**5A** and *trans*-**5B**, in the crystal. The selected bond lengths and angles are listed in Table 3. In both *trans*-**5A** and *trans*-**5B**, the coordination sphere displays a square-planar geometry. The Pt−N(benzonitrile) bond (1.969(3) Å for **5A**) is shorter than the Pt−N(pyridine) bond (2.013(3) Å for **5A**), which is consistent with the shorter Pt−N bonds found in other platinum complexes based on nitrile ligands.[19] The coordination plane forms dihedral angles of 84.39 and 66.58° with the pyridyl ring and the benzonitrile's phenyl ring, respectively, in **5A**. For molecule *trans*-**5B**, the dihedral angles are 72.93 and 40.79°, respectively, whereas in the crystal structure of *trans*-$Pt(PhCN)_2Cl_2$, the phenyl rings are essentially coplanar with the plane of the coordination sphere.[19a,b]

Further reaction of *trans*-**5** could either be the second ligand exchange with L^1 to give *trans*-**1** or the C−H activation to produce a cyclometalated complex. Refluxing *trans*-**5** in DCE led to decomposition of platinum complexes, as indicated by TLC, which showed a large dark-brown unmovable spot on the spotting line. Perhaps a more meaningful experiment is to examine the competition between C−H activation and ligand exchange reaction of *trans*-**5** in the presence of excess L^1 because a large excess amount of the substrate is used in the catalytic reaction. The reaction of *trans*-**5** with L^1 (molar ratio of *trans*-**5**/L^1 = 1:2) in DCE was very slow, but after 24 h, the reaction produced a mixture of *cis*-**1**, *trans*-**1**, *trans*-**2**, and remaining *trans*-**5** in 11, 12, 19, and 32% yield, respectively (^1H NMR analysis, Figure S12). Some decomposition of platinum complexes was also observed based on TLC analysis. Under the same conditions (molar ratio of substrate/L^1 = 1:2, DCE, reflux, 24 h), the reaction of *trans*-**1** gave a mixture of *trans*-**2** and remaining *trans*-**1** in 30 and 58% yield, respectively (^1H NMR analysis, Figure S13), while the reaction of *cis*-**1** produced a mixture of *trans*-**2**, *trans*-**1**, and remaining *cis*-**1** in 41, 9, and 29% yield, respectively (^1H NMR analysis, Figure S14). In both cases, the amount of free L^1 was increased by about 10−15% at the end of reaction, indicating the decomposition of platinum complexes. These results indicate that the intramolecular C−H activation of *trans*-**5** is competing with but not faster than the ligand substitution, especially in the presence of a large excess amount of L^1 under the catalytic conditions. The C−H activation of *cis*-**1** is faster than that of *trans*-**5** and *trans*-**1**. It is noteworthy that the ligand exchange of *trans*-**5** with L^1 also produced *cis*-**1**, indicating that isomerization of *trans*-**5** to *cis*-**5** may occur under the reaction conditions if the ligand exchange is stereospecific. The C−H activation of the formed *cis*-**1** may also contribute to the formation of *trans*-**2** in the reaction of *trans*-**5**. Although *cis*-**5** should be formed in the reaction of *cis*-$Pt(PhCN)_2Cl_2$, the potential C−H activation of *cis*-**5** would not be competitive

https://doi.org/10.1021/acs.organomet.1c00377
Organometallics 2021, 40, 3158−3169

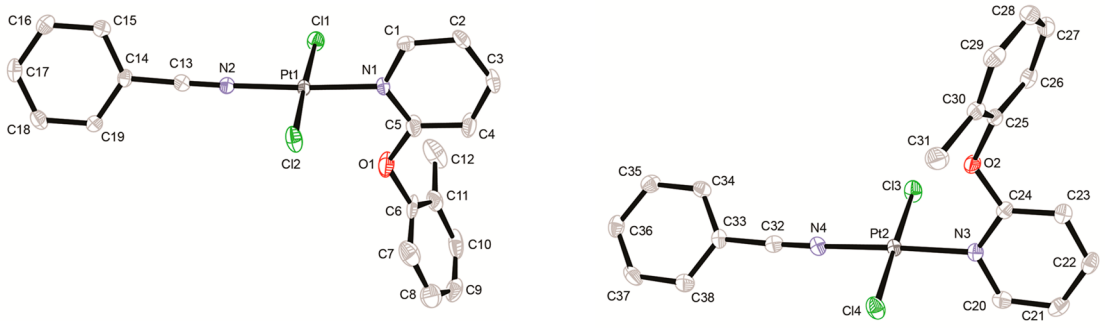

Figure 4. ORTEP diagram of complexes *trans*-**5A** (left) and *trans*-**5B** (right) shown with thermal ellipsoids given at the 50% probability level. Hydrogen atoms are omitted for clarity.

Table 3. Selected Bond Lengths (Å) and Angles (deg) for Compound *trans*-5

trans-**5A**		*trans*-**5B**	
Pt(1)−N(1)	2.013(3)	Pt(2)−N(3)	2.013(3)
Pt(1)−N(2)	1.969(3)	Pt(2)−N(4)	1.957(3)
Pt(1)−Cl(1)	2.2970(8)	Pt(2)−Cl(4)	2.2997(8)
Pt(1)−Cl(2)	2.3034(9)	Pt(2)−Cl(3)	2.3061(8)
N(2)−Pt(1)−N(1)	176.07(11)	N(4)−Pt(2)−N(3)	177.61(11)
N(2)−Pt(1)−Cl(1)	92.32(8)	N(4)−Pt(2)−Cl(4)	91.75(8)
N(1)−Pt(1)−Cl(1)	88.85(8)	N(3)−Pt(2)−Cl(4)	87.81(8)
N(2)−Pt(1)−Cl(2)	89.56(8)	N(4)−Pt(2)−Cl(3)	89.60(8)
N(1)−Pt(1)−Cl(2)	89.32(8)	N(3)−Pt(2)−Cl(3)	90.88(8)
Cl(1)−Pt(1)−Cl(2)	178.01(3)	Cl(4)−Pt(2)−Cl(3)	178.32(3)
C(13)−N(2)−Pt(1)	171.4(3)	C(32)−N(4)−Pt(2)	178.0(3)
Cl(1)−Pt(1)−N(1)−C(1)	85.72	Cl(3)−Pt(2)−N(3)−C(24)	72.88
Cl(2)−Pt(1)−N(1)−C(5)	83.39	Cl(4)−Pt(2)−N(3)−C(20)	72.83

because the ligand exchange with L^1 to form *cis*-**1** is much faster than the C−H activation (*cis*-**1**/*trans*-**2** = 10:1, Table 2).

Intramolecular C−H Activation/Cyclometalation of *cis*- and *trans*-1. We further compared the cycloplatination of *cis*- and *trans*-**1** in the absence of L^1 and controlled conditions, namely, using K_2CO_3 as a HCl scavenger, and the results are summarized in Table 4. In the presence of an excess amount of K_2CO_3, when a solution of *cis*-**1** in chlorobenzene was refluxed for 1 h, *trans*-**2** was formed in 55% yield. It was also found that, at this point, *cis*-**1** was completely isomerized to *trans*-**1**. Under the same reaction conditions, the reaction of *trans*-**1** only produced 26% of *trans*-**2** in 1 h. After 9 h, the C−H activation was complete in both cases. It is clear that the *cis* isomer is more reactive toward the intramolecular C−H activation. In a separate experiment, the cycloplatination reaction of *cis*-**1** was more carefully monitored, and it showed that C−H activation of *cis*-**1** was highly reactive and the isomerization of *cis*-**1** was competing. Within 15 min, all of *cis*-**1** was consumed and produced *trans*-**2** in 54% yield, along with 24% yield of *trans*-**1** due to isomerization. The yield of *trans*-**2** was only increased to 58 and 59% at 30 min and 1 h, respectively. The decomposition of platinum complexes to release free ligand L^1 was also observed in both reactions.

Table 4. Product Yields and Distribution for C−H Activation Reactions of *cis*- and *trans*-1[a]

cis-**1** or trans-**1** $\xrightarrow[133\ ^{o}C]{PhCl}$ cis-**1** + trans-**1** + trans-**2** + L^1 + others

reactant	*cis*-**1**				*trans*-**1**		
products	*trans*-**2**	*cis*-**1**	*trans*-**1**	L^1	*trans*-**2**	*trans*-**1**	L^1
1 h	55%	0	23%	10%	26%	61%	6%
2 h	54%		19%	10%	38%	42%	10%
3 h	58%		14%	10%	52%	28%	10%
4 h	64%		10%	10%	58%	22%	10%
5 h	67%		8%	10%	67%	15%	12%
9 h	71%		3%	14%	72%	8%	14%
separate run							
15 min	54%	0	24%	10%			
30 min	58%		23%	10%			
1 h	59%		23%	10%			

[a]Yields were estimated by analyzing ^{1}H NMR spectra of crude reaction mixtures, and the calculations were based on the integrations of the 6-Hs of the pyridine rings of the complexes and the ligand L^1 (Figure S15).

We could not detect the formation of *cis* cyclometalated complex *cis*-**2** in above reactions; however, we cannot rule out the formation of this isomer. A possible reason might be that the *trans*-**2** may be more stable than its *cis* isomer, and under the reaction conditions, *cis*-**2** can easily isomerize to more stable *trans*-**2**. We performed DFT calculations to assess the relative stability of the two isomers. The optimized geometries are shown in Figure 5, and the structural data are listed in Table 5. The optimized geometry of *trans*-**2** matches the molecular structure determined by the X-ray crystallography. Both *cis* and *trans* isomers display a boat-shape six-membered platinacycle. The distance of Pt and O to the plane of the boat-bottom are 0.644 and 0.396 Å for *trans*-**2**, respectively, and 0.696 and 0.410 Å for *cis*-**2**, respectively. The calculations also revealed that the *trans*-**2** is indeed more stable than *cis*-**2** by 4.43 kcal/mol, which indicates that even if at equilibrium

https://doi.org/10.1021/acs.organomet.1c00377
Organometallics 2021, 40, 3158−3169

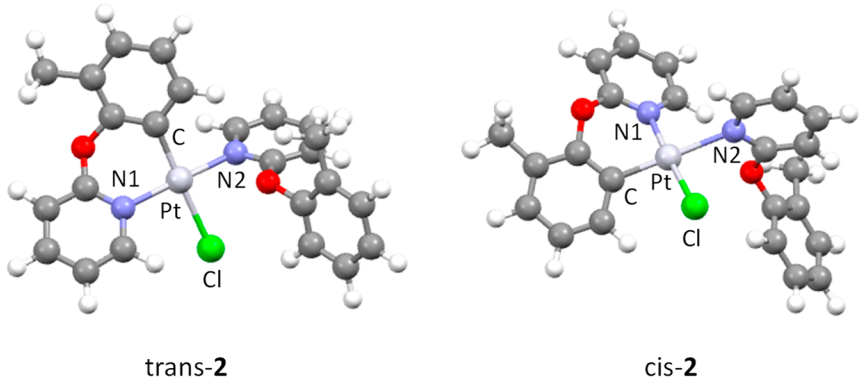

Figure 5. DFT-optimized geometries of *trans*-**2** and *cis*-**2**.

Table 5. Bond Lengths (Å) and Angles (deg) of Optimized Geometries of *trans*-2 and *cis*-2

cis-**2**		*trans*-**2**		
	calculated		calculated	X-ray
Pt−C	1.959	Pt−C	1.971	1.988
Pt−N1	2.056	Pt−N1	2.046	2.011
Pt−N2	2.265	Pt−N2	2.058	2.037
Pt−Cl	2.333	Pt−Cl	2.473	2.412
C−Pt−Cl	94.43	C−Pt−Cl	178.14	176.9
N1−Pt−N2	93.36	N1−Pt−N2	177.04	177.24
C−Pt−N1	88.56	C−Pt−N1	89.13	86.93
C−Pt−N2	176.28	C−Pt−N2	92.36	92.68
N1−Pt−Cl	177.00	N1−Pt−Cl	92.59	92.13
N2−Pt−Cl	83.68	N2−Pt−Cl	85.89	88.12

(about 132 °C, at reflux in chlorobenzene), the ratio of *trans*- and *cis*-**2** would be 99.6:0.4 in the reaction mixture.

Acylation of Cyclometalated Platinum Complex *trans*-2. The reaction of the cyclometalated platinum complex with ethyl chlorooxoacetate in chlorobenzene under reflux was too fast and caused severe degradation of reactants/products. The reaction mixture quickly turned dark brown, and the ^{1}H NMR spectrum of the reaction mixture was very messy. Therefore, we used DCE as the solvent, and at reflux, the acylation reaction proceeded smoothly to produce *cis*-**3** and *trans*-**3**, as well as *trans*-**1** as the major products (Scheme 6). The formation of *trans*-**1** can be attributed to the protonolysis of *trans*-**2** by the inevitable presence of HCl in the acylating reagent. The fast acylation reaction suggests that the acylation step is not the rate-determining step in the catalytic acylation reaction of $\mathbf{L}^1$ with ethyl chlorooxoacetate as C−H activation in DCE was very slow, as discussed above. The formation of *cis*-**3** is very interesting as the coordination configuration in *trans*-**2** was not retained during acylating step. The monitoring of the reaction showed that the ratio of *cis*-**3** to *trans*-**3** was about 1:3 and remained unchanged as the reaction time increased, which suggests that the reaction was under kinetic control. In fact, no isomerization of *cis*-**3** to *trans*-**3** was observed when heating a solution of *cis*-**3** in DCE at reflux.

The reaction of *cis*-**3** with 2 equiv of ligand $\mathbf{L}^1$ in chlorobenzene at reflux was complete in 1.5 h, producing a mixture of *trans*-**1** and *trans*-**2** in a 1:6 ratio (Figure S16) and releasing the acylated ligand $\mathbf{L}^2$ (Scheme 7), which completes the catalytic cycle. The similar reaction of *trans*-**3** with ligand $\mathbf{L}^1$ was very sluggish, with only about 50% conversion after 8 h and produced *trans*-**2** and acylated ligand $\mathbf{L}^2$ of about equal molar amounts (Figure S17), which indicates that the C−H activation is faster than the ligand exchange and the ligand exchange reaction may be the rate-limiting step. Again, the faster ligand exchange reaction with the *cis* isomer is notable. At lower temperature, when refluxing the mixture of $\mathbf{L}^1$ and *cis*-**3** in DCE for 1 h, no appreciable amount of ligand exchange product, neither *cis*-**1** nor *trans*-**1**, was detected.

Catalytic Activity of the Intermediate Platinum Complexes. In principle, if an intermediate platinum complex is involved in the catalytic cycle, it should effectively catalyze the C−H acylation, as well. Therefore, we investigated the catalytic activity of *cis*-**1**, *trans*-**1**, *trans*-**2**, *trans*-**5**, *cis*-**3**, and *trans*-**3** in the C−H acylation reaction of $\mathbf{L}^1$, especially compared the catalytic activity of the pairs of *cis* and *trans* isomers. The results are shown in Figures 6 and 7. It can be seen from Figures 6 and 7 that the *cis* complexes demonstrated much higher catalytic activity than their corresponding *trans* isomers, especially in the initial stage of the reaction. At 1 h, in the *cis*-**1**- and *cis*-**3**-catalyzed reactions, acylated product $\mathbf{L}^2$ was produced in 83 and 73% yield, respectively; however, in the *trans*-**1**- and *trans*-**3**-catalyzed reactions, $\mathbf{L}^2$ was produced only in about 5% yield. The catalytic activity of the cyclometalated platinum complex *trans*-**2** was between those of *cis*-**1** and *trans*-

Scheme 6. Acylation of *trans*-2 with Ethyl Chlorooxoacetate

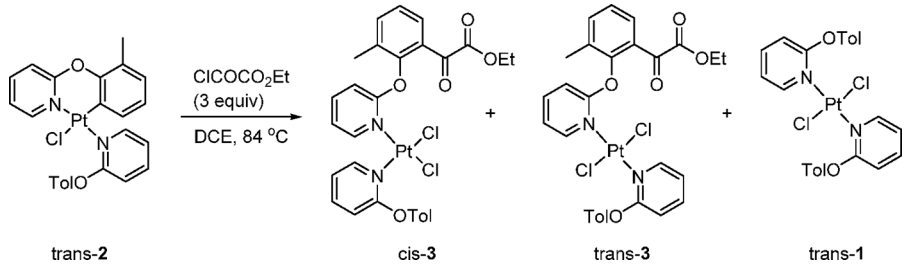

https://doi.org/10.1021/acs.organomet.1c00377
Organometallics 2021, 40, 3158−3169

Scheme 7. Reaction of *cis*-3 with Ligand L^1

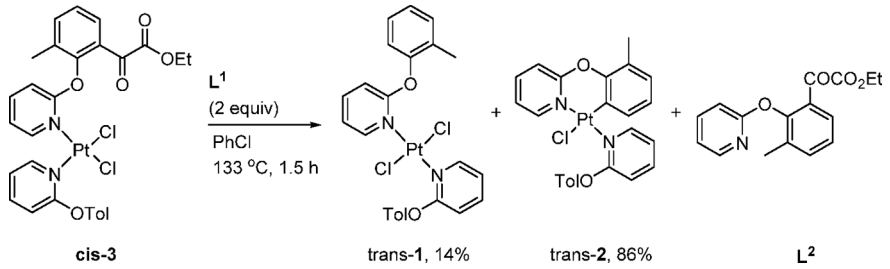

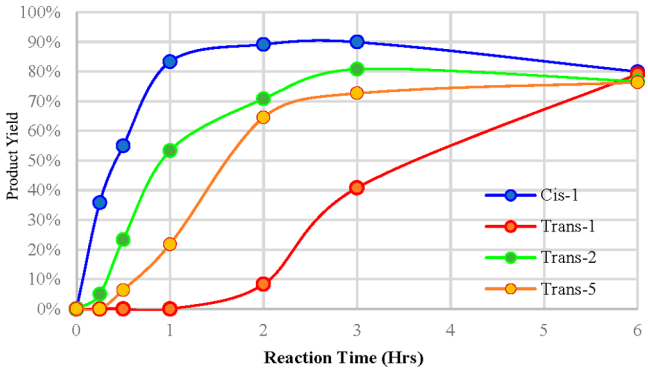

Figure 6. Comparison of catalytic activity of *cis*-**1**, *trans*-**1**, *trans*-**2**, and *trans*-**5** in the catalytic C−H acylation reaction. Data reported are based on single runs. For ease of readability, a smooth curve is added to connect the points using a graphing program but not intended to suggest any accurate kinetic features of the reaction.

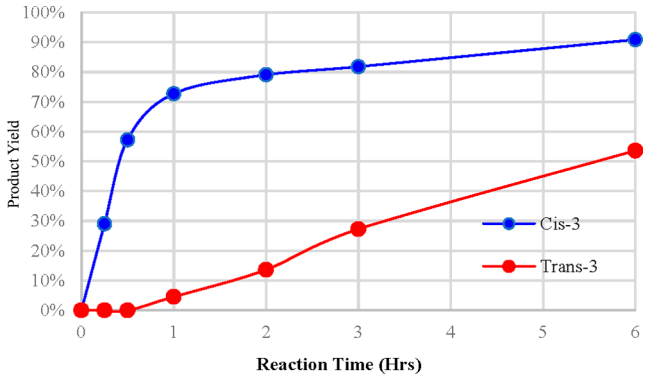

Figure 7. Comparison of catalytic activity of *cis*-**3** and *trans*-**3** in the catalytic C−H acylation reaction. Data reported are based on single runs. For ease of readability, a smooth curve is added to connect the points using a graphing program but not intended to suggest any accurate kinetic features of the reaction.

1, with the formation of L^2 in 53% after 1 h. Such a moderate catalytic activity of *trans*-**2** can be attributed to the two facts: (i) the acylation of *trans*-**2** produced both *cis*-**3** and *trans*-**3**, and (ii) *cis*-**3** demonstrated a high catalytic activity which is comparable to that of *cis*-**1**. The moderate catalytic activity of *trans*-**2** (lower than that of *cis*-**1** and *cis*-**3** but higher than that of *trans*-**1**) also indicates that the isomerization of *cis*-**2** to *trans*-**2** is highly competitive but not necessarily faster than the acylation of *cis*-**2** and implies the formation of *cis*-**2** in the intramolecular C−H activation of *cis*-**1**. Complex *trans*-**5** displays a catalytic activity lower than that of *cis*-**1** and *trans*-**2** but higher than that of *trans*-**1**, leading to the formation of L^2 in 22% yield at 1 h. This is easy to understand because the reaction of *trans*-**5** with L^1 generates both *cis*-**1** and *trans*-**1**, and intramolecular C−H activation of *trans*-**5** may also be competitive. Complex *trans*-**3** demonstrated the lowest catalytic activity among all platinum complexes evaluated here, possibly due to the rate-limiting ligand exchange of *trans*-**3** with substrate L^1 as mentioned above.

The increasing catalytic activity of the *trans* isomers in the later stage of the reaction is also noticeable. Especially in the case of *trans*-$Pt(PhCN)_2Cl_2$ and *trans*-**1**-catalyzed reactions, after 3−6 h, the yields of the product L^2 became comparable to those of the reactions catalyzed by their *cis* isomers. This can be reasonably explained by the access to the intermediate *cis*-platinum complexes during the reaction, namely, the formation of *cis*-**1** in the ligand exchange of *trans*-$(PhCN)_2Cl_2$ with substrate L^1 and the formation of small amount of *cis*-**3** in the acylation of cycloplatinated compound *trans*-**2**. Taking a further look at the extremely low catalytic activity of *trans*-**1** and *trans*-**3** at the initial stage, it is possible that the access to a *cis* complex, even in a small amount, effectively activates the catalytic process. Therefore, it is believed that there exists a fast pathway via all *cis* intermediates, *cis*-$Pt(PhCN_2)_2Cl_2$ → *cis*-**1** → *cis*-**2** → *cis*-**3**, which is, if not solely, mainly responsible for the efficient Pt-catalyzed C−H acylation of 2-aryloxypyridines with ethyl chlorooxoacetate. Another competing pathway is *cis*-$Pt(PhCN_2)_2Cl_2$ → *cis*-**1** → *cis*-**2** → *trans*-**2** → *cis*-**3**.

CONCLUSIONS

The platinum-catalyzed C−H acylation of 2-aryloxypyridines represents a rare case of ligand-directed C−H functionalization through a platinacycle intermediate. Studies of a series of stoichiometric reactions connect key reaction steps and furnish a catalytic cycle, which provide a strong support for the proposed reaction mechanism. The *cis*-platinum complexes, including the precatalyst *cis*-$Pt(PhCN)_2Cl_2$ and intermediate platinum complexes, exhibit remarkably higher reactivity toward the ligand exchange and the intramolecular C−H activation reactions when compared with that of their corresponding *trans* isomers, which reasonably explains the higher catalytic activity demonstrated by the *cis* isomers. However, the *cis* → *trans* isomerization is also competitive, suggesting multiple reaction pathways in the catalytic reaction (Scheme 8). The results indicate that the fast reaction pathway via all *cis*-platinum complexes, *cis*-$Pt(PhCN_2)_2Cl_2$ → *cis*-**1** → *cis*-**2** → *cis*-**3**, is responsible for the efficient catalytic C−H acylation reaction, although *cis*-**2** has not been isolated and tested. Since the isomerization of *cis*-**2** to *trans*-**2** is highly competitive, another fast pathway could be *cis*-$Pt(PhCN_2)_2Cl_2$ → *cis*-**1** → *cis*-**2** → *trans*-**2** → *cis*-**3**. To compare the reactivity of *cis*-**2** and *trans*-**2** in the acylation reaction may require a theoretical approach[20] as *cis*-**2** is not experimentally accessible. The formation of both coordination platinum complexes *cis*-**3**

https://doi.org/10.1021/acs.organomet.1c00377
Organometallics 2021, 40, 3158−3169

Scheme 8. Multiple Reaction Pathways in the Pt-Catalyzed C−H Acylation Reaction

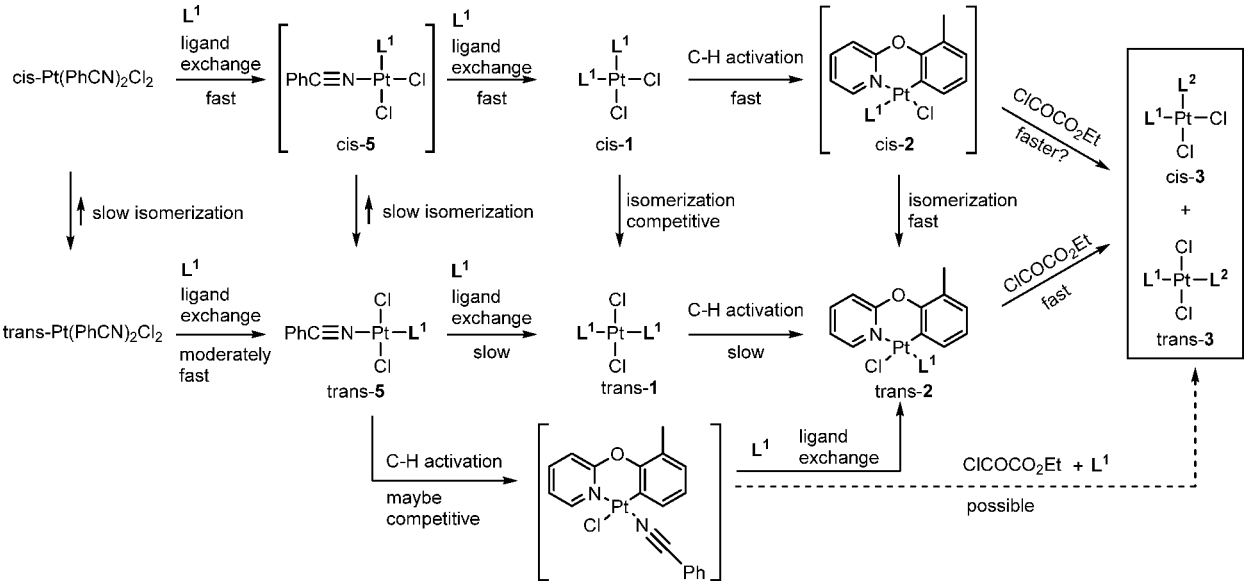

and *trans*-**3** from the acylation of cycloplatinated complex *trans*-**2** also allows regaining of a *cis*-platinum complex to revive the catalytic cycle.

EXPERIMENTAL SECTION

General Experimental Methods. All reactions involving moisture- and/or oxygen-sensitive compounds were carried out under an argon atmosphere and anhydrous conditions. All anhydrous solvents used were purchased and used as received. *cis*-Pt(PhCN)$_2$Cl$_2$[21] and *trans*-Pt(PhCN)$_2$Cl$_2$[22] were prepared according to literature procedures and purified by column chromatography if necessary. 2((2-Methylphenoxy))pyridine (**L^1**) and 2-phenoxypyridine (**L^3**) were prepared according to literature procedure.[23] All other reagents were purchased and were used as received. Thin layer chromatography was performed with silica gel 60 F_{254} plates. ^{1}H and ^{13}C NMR spectra were recorded on a Bruker 400 MHz spectrometer at 298 K using $CDCl_3$ or CD_2Cl_2 as the solvent. Chemical shifts were reported relative to TMS (0.0 ppm) and chloroform-*d* (77.0 ppm for C). Elemental analyses were performed at Atlantic Microlab, Norcross, GA.

Comparison of Catalytic Activity of *cis*- and *trans*-Pt(PhCN)$_2$Cl$_2$. General Procedure A. A 25 mL, three-neck round-bottom flask equipped with a condenser was dried and purged with argon and then charged with 2-(2-methylphenoxy)pyridine (**L^1**) (92.6 mg, 0.50 mmol), ethyl chlorooxoacetate (114 μL, 1.0 mmol), mesitylene (23 μL, 0.17 mmol, as the internal standard), and anhydrous chlorobenzene (3.0 mL). The mixture was stirred and heated to reflux under argon. After the reaction mixture reached reflux, a solution of *cis*-Pt(PhCN)$_2$Cl$_2$ (23.2 mg, 0.05 mmol) in 0.5 mL of chlorobenzene was added to the refluxing reaction mixture via a syringe. For NMR samplings at intervals, a 0.1 mL aliquot was taken by syringe and added to a 10 mL single-neck round-bottom flask equipped with a condenser. One drop of pyridine was added, and the reaction mixture was stirred and heated at 100 °C for 5 min to release the acylated ligand from the platinum. The crude mixture was then analyzed by ^{1}H NMR, and the yield of product **L^2** was calculated based on the internal standard (Figure S9).

Reaction of L^1 with *cis*-Pt(PhCN)$_2$Cl$_2$ in Chlorobenzene. General Procedure B. A 25 mL, three-neck round-bottom flask equipped with a condenser was charged with *cis*-Pt(PhCN)$_2$Cl$_2$ (236.1 mg, 0.5 mmol), **L^1** (277.9 mg, 1.5 mmol), and anhydrous chlorobenzene (4.0 mL). The mixture was stirred and heated at reflux for 2.5 h. The products, coordination complex *trans*-**1**, and cyclometalated complex *trans*-**2** were separated via column chromatography on silica gel with dichloromethane/ethyl acetate (20:1) as the eluting solvent.

*Complex Pt(**L^1**)$_2$Cl$_2$ (trans-**1**):* white solid, 130.7 mg, 41%; ^{1}H NMR (400 MHz, CD_2Cl_2) δ 8.75 (dd, J = 5.9, 1.8 Hz, 2H), 7.65 (td, J = 8.8, 1.8 Hz, 2H), 7.32−7.16 (m, 8H), 7.03 (t, J = 6.4 Hz, 2H), 6.51 (d, J = 8.5 Hz, 2H), 2.31 (s, 6H); ^{13}C NMR (100 MHz, CD_2Cl_2) δ 164.7, 153.2, 152.4, 141.5, 132.4, 131.4, 128.1, 126.7, 121.6, 119.5, 111.4, 16.5. Anal. Calcd for $C_{24}H_{22}Cl_2N_2O_2Pt$: C, 45.29; H, 3.48; N, 4.40. Found: C, 44.99; H, 3.72; N, 4.40.

*Cyclometalated Complex trans-**2**:* 126.4 mg, 42%; ^{1}H NMR (400 MHz, CD_2Cl_2) δ 9.38 (dd, J = 6.2, 1.6 Hz, 1H), 8.82 (dd, J = 5.9, 1.5 Hz, 1H), 7.85 (td, J = 8.7, 1.9 Hz, 1H), 7.77 (td, J = 8.9, 1.9 Hz, 1H), 7.29 (m, 1H), 7.23−7.19 (m, 3H), 7.06 (td, J = 7.2, 1.2 Hz, 1H), 7.00 (td, J = 7.4, 1.4 Hz, 1H), 6.90−6.84 (m, 2H), 6.64 (t, J = 7.4 Hz, 1H), 6.48−6.39 (m, 2H), 2.40 (s, 3H), 2.05 (s, 3H); ^{13}C NMR (100 MHz, CD_2Cl_2) δ 164.0, 160.4, 152.9, 152.5, 152.3, 151.8, 141.3, 141.1, 133.1, 132.4, 131.4, 128.3, 127.0, 126.6, 125.5, 124.4, 121.8, 119.7, 119.6, 115.8, 115.5, 111.1, 17.0, 16.0. Anal. Calcd for $C_{24}H_{21}ClN_2O_2Pt$: C, 48.05; H, 3.53; N, 4.67. Found: C, 48.30; H, 3.71; N, 4.61.

Reaction of L^1 with *trans*-Pt(PhCN)$_2$Cl$_2$ in Chlorobenzene. Following general procedure B, the reaction mixture was refluxed for 6 h for a complete conversion. Products *trans*-**1** and *trans*-**2** were isolated in 45 and 32% yields, respectively.

Alternative Synthesis of *trans*-1. A 50 mL, single-necked round-bottom flask equipped with a condenser and then charged with **L^1** (189.7 mg, 1.02 mmol), *cis*-Pt(PhCN)$_2$Cl$_2$ (230.9 mg, 0.49 mmol), and anhydrous chlorobenzene (8 mL). The mixture was stirred and heated at reflux for 1 h. A few drops of concentrated HCl were added to the reaction, and the mixture was stirred and heated at reflux for 1 h. After being cooled to room temperature and concentrated via a rotary evaporator, the product was precipitated with the addition of hexanes and afforded *trans*-**1** as a white solid, 256.3 mg, 82%.

Synthesis of *trans*-Pt(L^3**)$_2$Cl$_2$ (*trans*-4).** Following the procedure for the synthesis of *trans*-**1**, *trans*-**4** was obtained in 79% yield, yellow solid: ^{1}H NMR (400 MHz, $CDCl_3$) δ 8.77 (dd, J = 6.0, 1.6 Hz, 2H), 7.64−7.60 (m, 2H), 7.42−7.28 (m, 10H), 7.00 (t, J = 6.4 Hz, 2H), 6.62 (d, J = 8.3 Hz, 2H); ^{13}C NMR (100 MHz, $CDCl_3$) δ 165.0, 154.1, 152.7, 140.7, 130.2, 125.9, 121.3, 119.1, 112.1. Anal. Calcd for $C_{22}H_{18}Cl_2N_2O_2Pt$: C, 43.43; H, 2.98; N, 4.60. Found: C, 43.63; H, 2.93; N, 4.62.

Synthesis of *cis*-Pt(L^1**)$_2$Cl$_2$ (*cis*-1).** A 25 mL, single-neck round-bottom flask was charged with K_2PtCl_4 (415.7 mg, 1.00 mmol) and deionized H_2O (5.0 mL). This mixture was stirred to form a homogeneous solution. In a separate 25 mL, single-neck round-

https://doi.org/10.1021/acs.organomet.1c00377
Organometallics 2021, 40, 3158−3169

bottom flask, L^1 (749.0 mg, 4.04 mmol) was dissolved in glacial acetic acid (5.0 mL). This solution was then added to the aqueous solution of K_2PtCl_4, and the mixture was allowed to stir at room temperature for 5 days. The precipitates were collected via suction filtration, and the product was purified via column chromatography on silica gel with dichloromethane/ethyl acetate (v/v = 20:1) as the eluting solvent. Product *cis*-Pt(L^1)$_2$Cl$_2$ (*cis*-**1**) was obtained as a white solid, 248.3 mg, 38%: ^{1}H NMR (400 MHz, $CDCl_3$) δ 9.03 (d, J = 5.8 Hz, 2H), 7.62 (td, J = 7.5, 1.8 Hz, 2H), 7.27 (d, J = 7.5 Hz, 2H), 7.24−7.16 (m, 4H), 6.97 (t, J = 6.7 Hz, 2H), 6.63 (d, J = 7.7 Hz, 2H), 6.31 (d, J = 8.2, 2H), 1.97 (s, 6H); ^{13}C NMR (100 MHz, $CDCl_3$) δ 164.3, 154.1, 150.9, 140.9, 132.2, 130.4, 128.1, 126.9, 120.9, 119.2, 109.9, 15.8. Anal. Calcd for $C_{24}H_{22}Cl_2N_2O_2Pt$: C, 45.29; H, 3.48; N, 4.40. Found: C, 44.99; H, 3.50; N, 4.43.

Synthesis of *cis*-Pt(L^3)$_2$Cl$_2$ (*cis*-4). Following the procedure for the synthesis of *cis*-**1**, complex *cis*-**4** was obtained as a white solid in 41% yield. Crystals suitable for X-ray structure determination were grown by solvent diffusion in dichloromethane/hexanes: ^{1}H NMR (400 MHz, CD_2Cl_2) δ 8.95−8.92 (m, 2H), 7.74−7.71 (m, 2H), 7.46−7.42 (m, 4H), 7.36−7.32 (m, 2H), 7.05−7.01 (m, 2H), 6.82−6.80 (m, 2H), 6.56−6.54 (m, 2H); ^{13}C NMR (100 MHz, CD_2Cl_2) δ 164.4, 153.5, 153.0, 141.2, 130.6, 126.4, 120.3, 119.7, 111.4. Anal. Calcd for $C_{22.25}H_{18.5}Cl_{2.5}N_2O_2Pt$: C, 42.45; H, 2.96; N, 4.45. Found: C,.42.63; H, 2.96; N, 4.45.

Alternative Synthesis of Cyclometalated Complex *trans*-2. A 100 mL, single-necked round-bottom flask equipped with a condenser was charged with L^1 (466.4 mg, 2.52 mmol), *cis*-Pt(PhCN)$_2$Cl$_2$ (477.3 mg, 1.01 mmol), K_2CO_3 (1.24 mg, 8.98 mmol), and anhydrous chlorobenzene (18 mL). The mixture was stirred and heated at reflux for 2 h. After being cooled to room temperature and concentrated in vacuo, the product was purified via column chromatography on silica gel with dichloromethane/ethyl acetate (v/v = 25:1) as the eluting solvent, white solid, 386.0 mg, 64%. Crystals for X-ray crystallography were grown by slow evaporation in 1,2-dichloroethane.

Intramolecular C−H Activation/Cycloplatination of *cis*- and *trans*-1. A 25 mL, three-neck round-bottom flask equipped with a condenser was charged with *cis*-**1** (or *trans*-**1**) (31.8 mg, 0.05 mmol), potassium carbonate (49.8 mg, 0.30 mmol), and anhydrous chlorobenzene (3.0 mL). The mixture was stirred and heated at reflux. For sampling at intervals, a small aliquot (0.1 mL) of the crude reaction mixture was withdrawn from the reaction mixture by a syringe and analyzed by ^{1}H NMR.

Acylation Reaction of *trans*-2. A 25 mL, three-neck round-bottom flask equipped with a condenser was dried and purged with argon and then charged with *trans*-**2** (119.9 mg, 0.20 mmol), ethyl chlorooxoacetate (68 μL, 0.6 mmol), and anhydrous 1,2-dichloroethane (3.0 mL). The mixture was stirred and heated to reflux for 4 h. The mixture was cooled to room temperature and quenched with H_2O (5 mL). The aqueous layer was extracted with dichloromethane (3 × 15 mL). Combined organic layer was washed with saturated $NaHCO_3$ (1 × 15 mL), H_2O (2 × 15 mL), and brine (2 × 15 mL) and dried over anhydrous $MgSO_4$. The organic solution was filtered and concentrated via rotary evaporator, and products *trans*-Pt(L^1)(L^2)Cl$_2$ (*trans*-**3**) and *cis*-Pt(L^1)(L^2)Cl$_2$ (*cis*-**3**) were separated via column chromatography on silica gel with dichloromethane/ethyl acetate (v/v = 20:1), *trans*-**3**, yellow solid, 27.4% yield; *cis*-**3**, yellow solid, 11% yield.

cis-Pt(L^1)(L^2)Cl$_2$ (cis-3): ^{1}H NMR (400 MHz, $CDCl_3$) δ 9.02 (dd, J = 5.9, 1.6 Hz, 1H), 8.87 (dd, J = 6.0, 1.7 Hz, 1H), 7.65 (d, J = 7.5 Hz, 1H), 7.62−7.57 (m, 2H), 7.51−7.46 (m, 1H), 7.41 (t, J = 7.7 Hz, 1H), 7.30−7.27 (m, 1H), 7.21−7.12 (m, 2H), 6.95−6.91 (m, 1H), 6.84−6.81 (m, 1H), 6.73 (d, J = 7.2 Hz, 1H), 6.30 (d, J = 8.5 Hz, 1H), 6.21 (d, J = 8.5 Hz, 1H), 4.38 (bs, 2H, signal not resolved), 2.30 (bs, 3H), 2.10 (s, 3H), 1.37 (t, J = 7.1 Hz, 3H); ^{13}C NMR (100 MHz, $CDCl_3$) δ 184.1, 164.3, 163.4, 162.7, 154.0, 153.6, 151.2, 149.3, 140.8, 140.5, 138.4, 132.0, 130.6, 130.4, 127.9, 126.9, 126.5, 120.9, 119.2, 118.9, 110.4, 109.0, 62.7, 16.3, 15.9, 14.1. Anal. Calcd for $C_{28}H_{26}Cl_2N_2O_5Pt$: C, 45.66; H, 3.56; N, 3.80. Found: C, 45.49; H, 3.78; N, 3.75.

trans-Pt(L^1)(L^2)Cl$_2$ (trans-3): ^{1}H NMR (400 MHz, $CDCl_3$) δ 8.85 (d, J = 4.7 Hz, 1H), δ 8.80 (d, J = 4.7 Hz, 1H), 7.74 (d, J = 7.8, 1H), 7.68−7.64 (m, 1H), 7.61−7.57 (m, 1H), 7.51 (d, J = 7.6 Hz, 1H), 7.35 (t, J = 7.6, 1H), 7.24−7.18 (m, 4H), 7.04−6.96 (m, 2H), 6.58 (d, J = 8.1 Hz, 1 H), 6.48 (d, J = 8.7 Hz, 1H), 4.28 (q, J = 6.6 Hz, 2H), 2.33 (s, 3H), 2.22 (s, 3H), 1.25 (t, J = 7.1 Hz, 3H); ^{13}C NMR (100 MHz, $CDCl_3$) δ 185.6, 164.2, 163.2, 162.5, 153.0, 152.9, 151.8, 150.4, 140.7, 140.3, 137.9, 132.1, 131.8, 130.8, 129.6, 128.6, 127.6, 126.5, 126.1, 121.3, 119.2, 118.8, 111.7, 110.7, 63.3, 17.6, 16.3, 13.8. Anal. Calcd for $C_{28}H_{26}Cl_2N_2O_5Pt$: C, 45.66; H, 3.56; N, 3.80. Found: C, 45.45; H, 3.50; N, 3.74.

Ligand Exchange Reactions of *cis*- or *trans*-Pt(PhCN)$_2$Cl$_2$ with L^1. A 25 mL, three-neck round-bottom flask equipped with a condenser was charged with *trans*-Pt(PhCN)$_2$Cl$_2$ (169.3 mg, 0.36 mmol), L^1 (223.7 mg, 1.21 mmol), and anhydrous 1,2-dichloroethane (2.0 mL). The mixture was stirred and heated at reflux, and the crude reaction mixture was periodically monitored by ^{1}H NMR.

Synthesis of *trans*-Pt(PhCN)(L^1)Cl$_2$ (*trans*-5). A 25 mL, three-neck round-bottom flask equipped with a condenser was charged with *trans*-Pt(PhCN)$_2$Cl$_2$ (236.0 mg, 0.50 mmol), L^1 (274.8 mg, 1.48 mmol), and anhydrous 1,2-dichloroethane (2.0 mL). The mixture was stirred and heated at reflux for 1.5 h. The monosubstituted coordination complex was isolated and purified via column chromatography on silica gel with dichloromethane/ethyl acetate (v/v = 100:1) as the eluting solvent. Complex *trans*-**5** was obtained as a light yellow solid, 52.3 mg, 19%: ^{1}H NMR (400 MHz, $CDCl_3$) δ 8.63 (dd, J = 6.0, 1.8 Hz, 1H), 7.76 (d, J = 8.4, 2H), 7.71−7.63 (m, 2H), 7.53 (t, J = 8.0 Hz, 2H), 7.33 (d, J = 6.9, 1H), 7.25−7.21 (m, 3H), 7.05−7.01 (m, 1H) 6.45 (d, J = 8.6, 1H) 2.34 (s, 3H); ^{13}C NMR (100 MHz, $CDCl_3$) δ 164.3, 152.1, 151.2, 141.4, 134.7, 133.5, 132.0, 131.0, 129.3, 127.9, 126.8, 121.8, 118.9, 117.0, 110.4, 109.9, 16.2. Anal. Calcd for $C_{19}H_{16}Cl_2N_2OPt$: C, 41.17; H, 2.91; N, 5.05. Found: C, 40.92; H, 2.78; N, 5.00.

Ligand Exchange Reactions of *cis*-3 and *trans*-3 with L^1. A 25 mL, three-neck round-bottom flask equipped with a condenser was charged with *cis*-**3** (or *trans*-**3**) (16.5 mg, 0.022 mmol), L^1 (7.7 mg, 0.044 mmol), and anhydrous chlorobenzene (1.0 mL). The mixture was stirred and heated to reflux for 1.5 h. The reaction mixture was concentrated via a rotary evaporator, and the crude mixture was analyzed by ^{1}H NMR.

COMPUTATIONAL SECTION

DFT Calculations. Geometry optimizations, energy calculations, and harmonic frequency calculations were carried out using Gaussian 16 (G16) program[24] at density functional theory level with M062X functional[25] and def2-TZVP basis set for Pt[26] and cc-pVDZ[27] for other atoms (M062X/def2-TZVP-Pt/cc-pVDZ). The solvent effects were simulated with the polarizable continuum model using the integral equation formalism variant.[28] All the computations in this work were completed at East Carolina University using Altix 4700 computer cluster.

X-ray Crystallography. All single crystals were grown using either the slow evaporation of a sample solution or the solvent diffusion method. A suitable crystal was selected and mounted on a glass fiber. All measurements were made using graphite-monochromated Mo Kα radiation (0.71073 Å) on a Bruker-AXS three-circle DUO diffractometer, equipped with a SMART Apex II CCD detector. In each case, initial space group determination was based on a matrix consisting of 36 frames. The data were reduced using SAINT+[29] and empirical absorption correction applied using SADABS.[30] Structures were solved using direct methods. Least-squares refinement for all structures was carried out on F^2. All non-hydrogen atoms were refined anisotropically. Hydrogen atoms were placed in calculated positions and allowed to be refined isotropically as riding models. Structure solutions, refinement, and the calculation of derived results were performed using the SHELX and SHELXLE computer programs.[31,32]

https://doi.org/10.1021/acs.organomet.1c00377
Organometallics 2021, 40, 3158−3169

■ ASSOCIATED CONTENT

Supporting Information

The Supporting Information is available free of charge at https://pubs.acs.org/doi/10.1021/acs.organomet.1c00377.

Crystal data and structure refinement, ^{1}H NMR and ^{13}C NMR spectra for all new compounds, examples of ^{1}H NMR spectra of crude reaction mixtures, and analysis of product yields and distribution (PDF)

Cartesian coordinates of *cis*-**2** and *trans*-**2** (XYZ)

Accession Codes

CCDC 2088286−2088289 contain the supplementary crystallographic data for this paper. These data can be obtained free of charge via www.ccdc.cam.ac.uk/data_request/cif, or by emailing data_request@ccdc.cam.ac.uk, or by contacting The Cambridge Crystallographic Data Centre, 12 Union Road, Cambridge CB2 1EZ, UK; fax: + 44 1223 336033.

■ AUTHOR INFORMATION

Corresponding Author

Shouquan Huo − *Department of Chemistry, East Carolina University, Greenville, North Carolina 27858, United States;* orcid.org/0000-0001-9516-4013; Email: huos@ecu.edu

Authors

Alexander Barham − *Department of Chemistry, East Carolina University, Greenville, North Carolina 27858, United States*

Justin Neu − *Department of Chemistry, East Carolina University, Greenville, North Carolina 27858, United States*

Cathleen L. Canter − *Department of Chemistry, East Carolina University, Greenville, North Carolina 27858, United States*

Robert D. Pike − *Department of Chemistry, College of William and Mary, Williamsburg, Virginia 23185, United States;* orcid.org/0000-0002-8712-0288

Yumin Li − *Department of Chemistry, East Carolina University, Greenville, North Carolina 27858, United States;* orcid.org/0000-0003-2183-5317

Complete contact information is available at: https://pubs.acs.org/10.1021/acs.organomet.1c00377

Author Contributions

[§]A.B. and J.N. contributed equally to this work.

Notes

The authors declare no competing financial interest.

■ ACKNOWLEDGMENTS

The authors would like to acknowledge the financial support by the National Science Foundation (NSF-CHE-1900102). J.N. is grateful to the financial support provided by the National Science Foundation REU program (NSF-CHE-1851844).

■ REFERENCES

(1) (a) Shilov, A. E.; Shul'pin, G. B. Activation of C-H Bonds by Metal Complexes. *Chem. Rev.* **1997**, *97*, 2879−2932. (b) Fekl, U.; Goldberg, K. I. Homogeneous Hydrocarbon C-H Bond Activation and Functionalization with Platinum. *Adv. Inorg. Chem.* **2003**, *54*, 259−320. (c) Lersch, M.; Tilset, M. Mechanistic Aspects of C-H Activation by Pt Complexes. *Chem. Rev.* **2005**, *105*, 2471−2526. (d) West, N. M.; Templeton, J. L. Approaches to Alkane Functionalization with Tp'Pt and (nacnac)Pt Reagents. *Can. J. Chem.* **2009**, *87*, 288−296. (e) Labinger, J. A.; Bercaw, J. E. The Role of Higher Oxidation State Species in Platinum-Mediated C-H Bond Activation and Functionalization. In *Higher Oxidation State Organopalladium and Platinum Chemistry*; Canty, A. J., Ed.; Springer: Heidelberg, 2011; pp 29−60. (f) Zhou, M.; Crabtree, R. H. C-H Oxidation by Platinum Group Metal Oxo or Peroxo Species. *Chem. Soc. Rev.* **2011**, *40*, 1875−1884. (g) Vedernikov, A. N. Direct Functionalization of M-C (M = PtII, PdII) Bonds Using Environmentally Benign Oxidants, O_2 and H_2O_2. *Acc. Chem. Res.* **2012**, *45*, 803−813. (h) Labinger, J. A. Platinum-Catalyzed C-H Functionalization. *Chem. Rev.* **2017**, *117*, 8483−8496. (i) Gunsalus, N. J.; Koppaka, A.; Park, S. H.; Bischof, S. M.; Hashiguchi, B. G.; Periana, R. A. Homogeneous Functionalization of Methane. *Chem. Rev.* **2017**, *117*, 8521−8573. (j) Huo, S. Platinum in Chemistry: An Adventure from Phosphorescent Materials to Catalytic C-H Functionalization. *Chem. Rec.* **2018**, *18*, 1583−1595.

(2) (a) Lyons, T. W.; Sanford, M. S. Palladium-Catalyzed Ligand-Directed C(H Functionalization Reactions. *Chem. Rev.* **2010**, *110*, 1147−1169. (b) Colby, D. A.; Bergman, R. G.; Ellman, J. A. Rhodium-Catalyzed CRC Bond Formation via Heteroatom-Directed CCH Bond Activation. *Chem. Rev.* **2010**, *110*, 624−655. (c) Rouquet, G.; Chatani, N. Catalytic Functionalization of C(sp^2))H and C(sp^3)) H Bonds by Using Bidentate Directing Groups. *Angew. Chem., Int. Ed.* **2013**, *52*, 11726−11743.

(3) For functionalization of other cyclometalated complexes, see: (a) Dehand, J.; Pfeffer, M. Cyclometallated Compounds. *Coord. Chem. Rev.* **1976**, *18*, 327−352. (b) Ryabov, A. D. Cyclopalladated Complexes in Organic Synthesis. *Synthesis* **1985**, *1985*, 233−252. (c) Pfeffer, M. Reactions of Cyclopalladated Compound and Alkynes: New Pathways for Organic Synthesis? *Rec. Trav. Chim. Payes-Bas* **1990**, *109*, 567−576. (d) Omae, I. Three Types of Reactions with Intramolecular Five-Membered Ring Compounds in Organic Synthesis. *J. Organomet. Chem.* **2007**, *692*, 2608−2632.

(4) Huo, S.; Carroll, J.; Vezzu, D. A. K. Design, Synthesis, and Applications of Highly Phosphorescent Cyclometalated Platinum Complexes. *Asian J. Org. Chem.* **2015**, *4*, 1210−1245.

(5) Williams, N. A.; Uchimaru, Y.; Tanaka, M. Platinum Catalyzed Regioselective ortho-Silylation of Benzylideneamines *via* Intramolecular C-H Activation. *J. Chem. Soc., Chem. Commun.* **1995**, 1129−1130.

(6) (a) Carroll, J.; Gagnier, J. P.; Garner, A. W.; Moots, J. G.; Pike, R. D.; Li, Y.; Huo, S. Reaction of N-Isopropyl-N-phenyl-2,2′-bipyridin-6-amine with K_2PtCl_4: Selective C-H Bond Activation, C-N Bond Cleavage, and Selective Acylation. *Organometallics* **2013**, *32*, 4828−4836. (b) Carroll, J.; Woolard, H. G.; Mroz, R.; Nason, C. A.; Huo, S. Regiospecific Acylation of Cycloplatinated Complexes: Scope, Limitations, and Mechanistic Implications. *Organometallics* **2016**, *35*, 1313−1322.

(7) (a) McAteer, D. C.; Javed, E.; Huo, L.; Huo, S. Platinum-Catalyzed Double Acylation of 2-(Aryloxy)pyridines via Direct C(H Activation. *Org. Lett.* **2017**, *19*, 1606−1609. (b) Javed, E.; Guthrie, J. D.; Neu, J.; Chirayath, G. S.; Huo, S. Introducing an α-Keto Ester Functional Group through Pt-Catalyzed Direct C-H Acylation with Ethyl Chlorooxoacetate. *ACS Omega* **2020**, *5*, 8393−8402.

(8) (a) de Geest, D. J.; O'Keefe, B. J.; Steel, P. J. Cyclometallated Compounds. XIII. Cyclopalladation of 2-Phenoxypyridine and Structurally-related Compounds. *J. Organomet. Chem.* **1999**, *579*, 97−105. (b) O'Keef, B. J.; Steel, P. J. Cyclometallated compounds. XVI. Double Cyclopalladations of Bis(2-pyridyloxy)naphthalenes. Kinetic versus Thermodynamic Control of Regiospecificity. *Organometallics* **2003**, *22*, 1281−1292.

(9) Garner, A. W.; Harris, C. F.; Vezzu, D. A. K.; Pike, R. D.; Huo, S. Solvent-Controlled Switch of Selectivity Between sp^2 and sp^3 C H Bond Activation by Platinum (II). *Chem. Commun.* **2011**, *47*, 1902−1904.

(10) (a) Zhang, F.; Kirby, C. W.; Hairsine, D. W.; Jennings, M. C.; Puddephatt, R. J. Activation of C-H Bonds of Arenes: Selectivity and Reactivity in Bis(pyridyl) Platinum(II) Complexes. *J. Am. Chem. Soc.* **2005**, *127*, 14196−14197. (b) Zhang, F.; Prokopchuk, E. M.; Broczkowski, M. E.; Jennings, M. C.; Puddephatt, R. J.

Hydridodimethylplatinum(IV) Complexes with Bis(pyridine) Ligands: Effect of Chelate Ring Size on Reactivity. *Organometallics* **2006**, *25*, 1583−1591.
(11) (a) Vezzu, D. A. K.; Deaton, J. C.; Jones, J. S.; Bartolotti, L.; Harris, C. F.; Marchetti, A. P.; Kondakova, M.; Pike, R. D.; Huo, S. Highly Luminescent Tetradentate Bis-cyclometalated Platinum Complexes: Design, Synthesis, Structure, Photophysics, and Electroluminescence Application. *Inorg. Chem.* **2010**, *49*, 5107−5119. (b) Ravindranathan, D.; Vezzu, D. A. K.; Bartolotti, L.; Boyle, P. D.; Huo, S. Improvement in Phosphorescence Efficiency Through Tuning of Coordination Geometry of Tridentate Cyclometalated Platinum (II) Complexes. *Inorg. Chem.* **2010**, *49*, 8922−8928. (c) Harris, C. F.; Vezzu, D. A. K.; Bartolotti, L.; Boyle, P. D.; Huo, S. Synthesis, Structure, Photophysics, and a DFT Study of Phosphorescent C*N̂N- and ĈNN-Coordinated Platinum Complexes. *Inorg. Chem.* **2013**, *52*, 11711−11722. (d) Huo, S.; Harris, C. F.; Vezzu, D. A. K.; Gagnier, J. P.; Smith, M. E.; Pike, R. D.; Li, Y. Novel Phosphorescent Tetradentate Bis-Cyclometallated ĈC*N̂N-Coordinated Platinum Complexes: Structure, Photophysics, and a Synthetic adventure. *Polyhedron* **2013**, *52*, 1030−1040.
(12) Hartley, F. R. *The Chemistry of Platinum and Palladium*; Wiley: New York, 1973; pp 490−519.
(13) (a) Appleton, T.G.; Clark, H.C.; Manzer, L.E. The *trans*-Influence: Its measurement and Significance. *Coord. Chem. Rev.* **1973**, *10*, 335−422. (b) Hartley, F. R. The *cis*- and *trans*-Effects of Ligands. *Chem. Soc. Rev.* **1973**, *2*, 163−179. (c) Kapoor, P. N.; Kakkar, R. Trans and *cis* Influence in Square Planar Pt(II) Complexes: A Density Functional Study of $[PtClX(dms)_2]$ and Related Complexes. *J. Mol. Struct.: THEOCHEM* **2004**, *679*, 149−156.
(14) (a) Colamarino, P.; Orioli, P. L. Crystal and Molecular Structures of *cis*- and *trans*-Dichlorobispyridine-platinum(II). *J. Chem. Soc., Dalton Trans.* **1975**, 1656−1659. (b) Lewis, N. A.; Pakhomova, S.; Marzilli, P. A.; Marzilli, L. G. Synthesis and Characterization of Pt(II) Complexes with Pyridyl Ligands: Elongated Octahedral Ion Pairs and Other Factors Influencing ^{1}H NMR Spectra. *Inorg. Chem.* **2017**, *56*, 9781−9793.
(15) Umezawa, Y.; Tsuboyama, S.; Honda, K.; Uzawa, J.; Nishio, M. CH/π Interaction in the Crystal Structure of Organic Compounds. A Database Study. *Bull. Chem. Soc. Jpn.* **1998**, *71*, 1207−1213.
(16) Cross, R. J. Ligand Substitution Reactions of Square-planar Molecules. *Chem. Soc. Rev.* **1985**, *14*, 197−223.
(17) (a) Cooper, M. K.; Downes, J. M. Substitution of a Platinum(I1) Complex without Retention of Stereochemistry; Direct Evidence for Pseudorotation of a Five-co-ordinate Platinum(II) Cationic Complex containing Chelating Phosphine Ligands. *J. Chem. Soc., Chem. Commun.* **1981**, 381−382. (b) Erickson, L. F.; Ferrett, T. A.; Buhse, L. F. Kinetics and Mechanisms of Ligand Exchange, Substitution, and Isomerization of Me_2SO-Amino Acid Complexes of Platinum(II): Evidence for a Pseudorotation Mechanism. *Inorg. Chem.* **1983**, *22*, 1461−1467.
(18) (a) Uchiyama, T.; Toshiyasu, Y.; Nakamura, Y.; Miwa, T.; Kawaguchi, S. The Isolation, Characterization, and Isomerization of *cis*- and *trans*-Bis(benzonitrile)dichloroplatinum(II). *Bull. Chem. Soc. Jpn.* **1981**, *54*, 181−185. (b) Kukushkin, V. Y.; Tkachuk, V. M. Z. Synthesis, Thermal Isomerization in Solution and in Solid Phase of the Complexes $[Pt(RCN)_2Cl_2]$. *Z. Anorg. Allg. Chem.* **1992**, *613*, 123−126.
(19) (a) Lauher, J. W.; Ibers, J. A. Synthesis of Diiminosuccinonitrile Complexes. Preparation and Structure of Bis(diiminosuccinonitrilo)-platinum(II) *trans*-Dichlorobis(benzonitrile)platinum(II). *Inorg. Chem.* **1975**, *14*, 640−645. (b) Eysel, H. H.; Guggolz, E.; Kopp, M.; Ziegler, M. L. Synthesis and Characterization of *cis*- and *trans*-Bis(benzonitrile)dichloroplatinum(IL). X-Ray Structure Analysis of Both the *cis*- and *trans*-Species. *Z. Anorg. Allg. Chem.* **1983**, *499*, 31−43. (c) Rochon, F. D.; Melanson, R.; Thouin, E.; Beauchamp, A. L.; Bensimon, C. Synthesis and Study of Pt(ll)-nitrile Complexes. Multinuclear NMR Spectra and Crystal Structures of Compounds of the Types $[Pt(R\text{-}CN)Cl_3]^-$ and *cis* and *trans*-$Pt(R\text{-}CN)_2Cl_2$. *Can. J. Chem.* **1996**, *74*, 144−152.
(20) Warden, E.; Bartolotti, L.; Huo, S.; Li, Y. Theoretical Probe to the Mechanism of Pt-Catalyzed C-H Acylation Reaction: Possible Pathways for the Acylation Reaction of a Platinacycle. *Inorg. Chem.* **2020**, *59*, 555−562.
(21) Kiyooka, S.-i.; Matsumoto, S.; Shibata, T.; Shinozaki, K.-i. Platinum(II) Complex-catalyzed Enantioselective Aldol Reaction with Ketene Silyl Acetals in DMF at Room Temperature. *Tetrahedron* **2010**, *66*, 1806−1816.
(22) Boutain, M.; Duckett, S. B.; Dunne, J. P.; Godard, C.; Hernandez, J. M.; Holmes, A. J.; Khazal, I. G.; Lopez-Serrano, J. A Parahydrogen Based NMR Study of Pt-Catalyzed Alkyne Hydrogenation. *Dalton Trans.* **2010**, *39*, 3495−3500.
(23) Maiti, D.; Buchwald, S. L. Cu-Catalyzed Arylation of Phenols: Synthesis of Sterically Hindered and Heteroaryl Diaryl Ethers. *J. Org. Chem.* **2010**, *75*, 1791−1794.
(24) Frisch, M. J.; Trucks, G. W.; Schlegel, H. B.; Scuseria, G. E.; Robb, M. A.; Cheeseman, J. R.; Scalmani, G.; Barone, V.; Petersson, G. A.; Nakatsuji, H.; Li, X.; Caricato, M.; Marenich, A. V.; Bloino, J.; Janesko, B. G.; Gomperts, R.; Mennucci, B.; Hratchian, H. P.; Ortiz, J. V.; Izmaylov, A. F.; Sonnenberg, J. L.; Williams-Young, D.; Ding, F.; Lipparini, F.; Egidi, F.; Goings, J.; Peng, B.; Petrone, A.; Henderson, T.; Ranasinghe, D.; Zakrzewski, V. G.; Gao, J.; Rega, N.; Zheng, G.; Liang, W.; Hada, M.; Ehara, M.; Toyota, K.; Fukuda, R.; Hasegawa, J.; Ishida, M.; Nakajima, T.; Honda, Y.; Kitao, O.; Nakai, H.; Vreven, T.; Throssell, K.; Montgomery, J. A., Jr.; Peralta, J. E.; Ogliaro, F.; Bearpark, M. J.; Heyd, J. J.; Brothers, E. N.; Kudin, K. N.; Staroverov, V. N.; Keith, T. A.; Kobayashi, R.; Normand, J.; Raghavachari, K.; Rendell, A. P.; Burant, J. C.; Iyengar, S. S.; Tomasi, J.; Cossi, M.; Millam, J. M.; Klene, M.; Adamo, C.; Cammi, R.; Ochterski, J. W.; Martin, R. L.; Morokuma, K.; Farkas, O.; Foresman, J. B.; Fox, D. J. *Gaussian 16*, revision B.01; Gaussian, Inc.: Wallingford, CT, 2016.
(25) Zhao, Y.; Truhlar, D. G. The M06 Suite of Density Functionals for Main Group Thermochemistry, Kinetics, Noncovalent Interactions, Excited States, and Transition Elements: Two New Functionals and Systematic Testing of Four M06 Functionals and Twelve Other Functionals. *Theor. Chem. Acc.* **2008**, *120*, 215−241.
(26) Weigend, F.; Ahlrichs, R. Balanced Basis Sets of Split Valence, Triple zeta Valence and Quadruple zeta Valence Quality for H to Rn: Design and Assessment of Accuracy. *Phys. Chem. Chem. Phys.* **2005**, *7*, 3297−3305.
(27) Dunning, T. H. Gaussian Basis Sets for Use in Correlated Molecular Calculations. I. The Atoms Boron through Neon and Hydrogen. *J. Chem. Phys.* **1989**, *90*, 1007−1023.
(28) Tomasi, J.; Mennucci, B.; Cammi, R. Quantum Mechanical Continuum Solvation Models. *Chem. Rev.* **2005**, *105*, 2999−3093.
(29) *SAINT PLUS*; Bruker Analytical X-ray Systems: Madison, WI, 2001.
(30) *SADABS*; Bruker Analytical X-ray Systems: Madison, WI, 2001.
(31) Sheldrick, G. M. Crystal structure refinement with SHELXL. *Acta Crystallogr., Sect. C: Struct. Chem.* **2015**, *71*, 3−8.
(32) Hubschle, C. B.; Sheldrick, G. M.; Dittrich, B. ShelXle: A Qt Graphical User Interface for SHELXL. *J. Appl. Crystallogr.* **2011**, *44*, 1281−1284.

https://doi.org/10.1021/acs.organomet.1c00377
Organometallics 2021, 40, 3158−3169